



## X-ray Analysis of the NMC-A $\beta$ -Lactamase at 1.64-Å Resolution, a Class A Carbapenemase with Broad Substrate Specificity

Peter Swarén, Laurent Maveyraud, Xavier Raquet, Stéphanie Cabantous, Colette Duez, Jean-Denis Pedelacq, Sophie Mariotte-Boyer, Lionel Mourey, Roger Labia, Marie-Hélène Nicolas-Chanoine, et al.

### ► To cite this version:

Peter Swarén, Laurent Maveyraud, Xavier Raquet, Stéphanie Cabantous, Colette Duez, et al.. X-ray Analysis of the NMC-A  $\beta$ -Lactamase at 1.64-Å Resolution, a Class A Carbapenemase with Broad Substrate Specificity. *Journal of Biological Chemistry*, 1998, 273 (41), pp.26714-26721. 10.1074/jbc.273.41.26714 . hal-03004553

**HAL Id: hal-03004553**

**<https://cnrs.hal.science/hal-03004553>**

Submitted on 20 Nov 2020

**HAL** is a multi-disciplinary open access archive for the deposit and dissemination of scientific research documents, whether they are published or not. The documents may come from teaching and research institutions in France or abroad, or from public or private research centers.

L'archive ouverte pluridisciplinaire **HAL**, est destinée au dépôt et à la diffusion de documents scientifiques de niveau recherche, publiés ou non, émanant des établissements d'enseignement et de recherche français ou étrangers, des laboratoires publics ou privés.

## X-ray Analysis of the NMC-A $\beta$ -Lactamase at 1.64-Å Resolution, a Class A Carbapenemase with Broad Substrate Specificity\*

(Received for publication, June 1, 1998, and in revised form, July 28, 1998)

Peter Swarén<sup>‡</sup>, Laurent Maveyraud<sup>‡</sup>, Xavier Raquet<sup>§</sup>, Stéphanie Cabantous<sup>‡</sup>, Colette Duez<sup>§</sup>, Jean-Denis Pédelacq<sup>‡</sup>, Sophie Mariotte-Boyer<sup>¶</sup>, Lionel Mourey<sup>‡</sup>, Roger Labia<sup>||</sup>, Marie-Hélène Nicolas-Chanoine<sup>\*\*</sup>, Patrice Nordmann<sup>‡‡</sup>, Jean-Marie Frère<sup>§</sup>, and Jean-Pierre Samama<sup>‡§§</sup>

From the <sup>‡</sup>Groupe de Cristallographie Biologique, Institut de Pharmacologie et de Biologie Structurale, UPR 9062 CNRS, 205 route de Narbonne, F-31077 Toulouse CEDEX, France, the <sup>§</sup>Centre d'Ingénierie des Protéines, Université de Liège, Institut de Chimie B6, Sart Tilman, B-4000 Liège, Belgium, the <sup>¶</sup>Service de Bactériologie-Virologie, Hôpital Lariboisière, 2 rue Ambroise Paré, F-75475 Paris CEDEX 10, France, the <sup>||</sup>Chimie et Biologie de Substances Actives, UMR 175 CNRS-MNH, 6 rue de l'Université, F-29000 Quimper, France, the <sup>\*\*</sup>Laboratoire de Microbiologie, Université Paris V, Faculté de Médecine Paris-Ouest, F-92100 Boulogne, France, and the <sup>‡‡</sup>Service de Bactériologie et de Virologie, Hôpital Bicêtre, F-94275 Le Kremlin Bicêtre, France

The treatment of infectious diseases by penicillin and cephalosporin antibiotics is continuously challenged by the emergence and the dissemination of the numerous TEM and SHV mutant  $\beta$ -lactamases with extended substrate profiles. These class A  $\beta$ -lactamases nevertheless remain inefficient against carbapenems, the most effective antibiotics against clinically relevant pathogens. A new member of this enzyme class, NMC-A, was recently reported to hydrolyze at high rates, and hence destroy, all known  $\beta$ -lactam antibiotics, including carbapenems and cephamycins. The crystal structure of NMC-A was solved to 1.64-Å resolution, and reveals modifications in the topology of the substrate-binding site. While preserving the geometry of the essential catalytic residues, the active site of the enzyme presents a disulfide bridge between residues 69 and 238, and certain other structural differences compared with the other  $\beta$ -lactamases. These unusual features in class A  $\beta$ -lactamases involve amino acids that participate in enzyme-substrate interactions, which suggested that these structural factors should be related to the very broad substrate specificity of this enzyme. The comparison of the NMC-A structure with those of other class A enzymes and enzyme-ligand complexes, indicated that the position of Asn-132 in NMC-A provides critical additional space in the region of the protein where the poorer substrates for class A  $\beta$ -lactamases, such as cephamycins and carbapenems, need to be accommodated.

The extensive use of  $\beta$ -lactam antibiotics has resulted in bacteria becoming resistant to these agents. The resistance is mainly mediated by the class A  $\beta$ -lactamases and is spread by plasmid exchanges encoding the TEM and SHV mutant en-

zymes (1). In nosocomial bacterial infections highly resistant to penicillins and cephalosporins, imipenem and other carbapenem antibiotics are often considered antibiotics of last resort. These compounds are active against almost all clinically important Gram-positive and Gram-negative pathogens, including  $\beta$ -lactamase producers (2), and were shown to be nearly ideal drugs in pediatrics (3). Carbapenems differ from the classical  $\beta$ -lactam antibiotics because of the presence of a carbapenem ring fused to the 4-membered  $\beta$ -lactam ring and by the presence of the 6 $\alpha$ -1R-hydroxyethyl substituent instead of the acylamido group found at 6 $\beta$  and 7 $\beta$  positions of penicillins and cephalosporins, respectively (Fig. 1). The antibacterial efficiency of carbapenems arises from several factors: (i) they are resistant to hydrolysis by nearly all class A  $\beta$ -lactamases, including the extended-spectrum mutant enzymes (4); (ii) carbapenemases, oxacillinases, and chromosomal cephalosporinases from different bacterial strains hydrolyze imipenem at very slow rates although the apparent binding constants are in the micromolar range (5, 6); and (iii) carbapenems display a very high affinity for the penicillin-sensitive pharmacological target enzymes (PBPs) involved in the final steps of the peptidoglycan cell wall synthesis (7).

Until recently, the only enzymes known to display high hydrolytic activity against carbapenems (carbapenemases) were the class B metallo- $\beta$ -lactamases (8, 9), and the high resolution x-ray structures of two such enzymes were recently reported (10, 11). Surprisingly, three highly homologous carbapenemases, NMC-A (12) and IMI-1 (13) from *Enterobacter cloacae*, and Sme-1 (14) from *Serratia marcescens*, belong to the class A family of  $\beta$ -lactamases (15), which have so far been characterized by their specificity for penicillins. NMC-A, IMI-1, and Sme-1 hydrolyze at significant rates a wide range of  $\beta$ -lactam antibiotics, including those usually considered as resistant to the class A enzymes (13, 16, 17). A preliminary x-ray analysis of Sme-1 has been reported (18). Here, we present the x-ray structure of NMC-A, solved to 1.64-Å resolution, and its comparison with those of the typical class A  $\beta$ -lactamases. The differences observed in the substrate-binding site, complemented with kinetic measurements, provide structural explanations for the broadened substrate profile of this enzyme.

### MATERIALS AND METHODS

**Protein Expression and Purification**—Oligonucleotides were purchased from Eurogentec (Belgium). To overexpress the NMC-A gene, an

\* The work in Liège was supported by the Belgian Program of Inter-university Poles of Attraction (PAI No. 19) and an Action Concertée with the Belgian Government (93–98/170). This work was also supported by the Actions Concertées Coordonnées des Sciences du Vivant and la Région Midi-Pyrénées. The costs of publication of this article were defrayed in part by the payment of page charges. This article must therefore be hereby marked "advertisement" in accordance with 18 U.S.C. Section 1734 solely to indicate this fact.

The atomic coordinates and structure factors (codes 1BUE and 1BUESF) have been deposited in the Protein Data Bank, Brookhaven National Laboratory, Upton, NY.

§§ To whom correspondence should be addressed. Tel.: 33-5-61-17-54-44; Fax: 33-5-61-17-54-48; E-mail: samama@ipbs.fr.

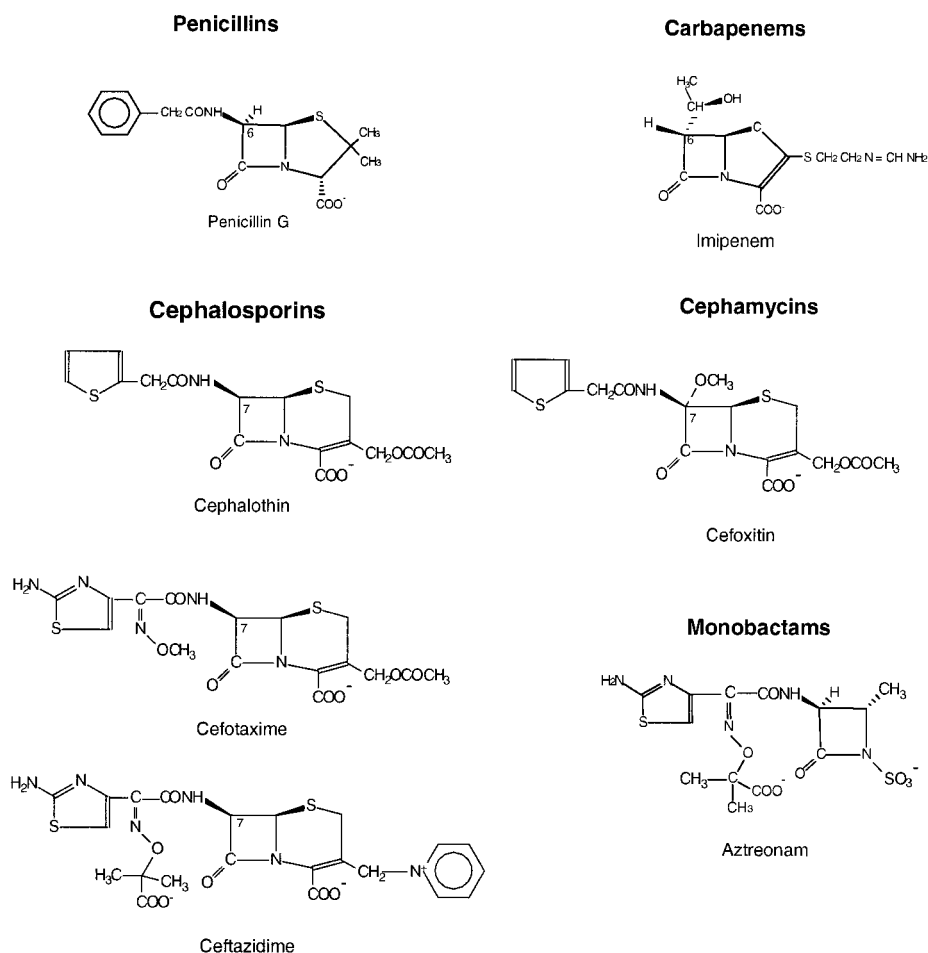


FIG. 1. Chemical structures of the five classes of  $\beta$ -lactam antibiotics. The letters *a*, *b*, and *c* indicate kinetic data from Refs. 16, 42, and 17, respectively. \*, not measurable.

$k_{cat}/K_m$ ( $mM^{-1}s^{-1}$ )	NMC-A <sup>a</sup>	TEM-1 <sup>b</sup>	TEM-19 <sup>b</sup> (Gly 238 Ser)
Penicillin G	9 300	84 000	10 000
Cephalothin	15 200	650	2 300
Cefotaxime	300	1.5	230
Ceftazidime	52	0.07	5
Imipenem	11 300	2.4 <sup>c</sup>	*
Cefoxitin	62	0.006 <sup>c</sup>	*
Aztreonam	5 600	0.7	1

800-base pair DNA fragment was amplified by PCR<sup>1</sup> using the Vent<sup>TM</sup> DNA polymerase (New England Biolabs, Beverly, MA), pPTN1 as template (12) and the following oligonucleotides as primers: 1) a 37-base sense primer: 5'-GAGGGTACCATATGTCACCTTAATGTAAAGCAAGTAG-3' with Asp-718 and *Nde*I restriction sites at the 5' end, and the 23 last bases encoding the N-terminal MSLNVKQS peptide of the preprotein; and 2) a 35-base antisense primer: 5'-GAGGGATCCTAG-GTTTATTTAAGGTTATCAATTGC-3' with a *Bam*HI restriction site at the 5' end, and the last 21 bases complementary to the sequence encoding the C-terminal AIDNLK peptide and to the TAA stop codon. The 800-base pair purified PCR fragment and pUC20 (Boehringer Mannheim) were digested with Asp-718 and *Bam*HI and ligated. The resulting plasmid was used to transform the *Escherichia coli* Top10F' cells (Invitrogen) and for mutagenesis purposes. The correct PCR fragment digested with *Nde*I and *Bam*HI was thereafter inserted into the pET22b(+) plasmid (Novagen) after modification of its ampicillin resistance by insertion of a kanamycin resistance cartridge (Amersham Pharmacia Biotech). The resulting supercoiled overexpression plasmid

was isolated from *E. coli* Top10F' and used to transform *E. coli* BL21DE3. Cells were grown at 37 °C in an 18-liter Bio-Laffite fermenter containing 15 liters of Luria-Bertani broth added with 50  $\mu$ g/ml of ampicillin. When the  $A_{550}$  reached 1.0, IPTG was added at a 0.5 mM final concentration, and the culture was continued for 3 h. The cells were collected by centrifugation, and the periplasmic content was liberated by lysozyme treatment. The supernatant was then dialyzed against 10 mM Tris-HCl buffer, pH 8.5, and loaded onto a Q-Sepharose Fast Flow column (4.6  $\times$  30 cm<sup>2</sup>) equilibrated with the same buffer. The enzyme was eluted with a linear NaCl gradient (0–250 mM final concentration) over 1 liter. Active fractions were pooled, dialyzed against 10 mM sodium phosphate buffer, pH 7.0, and loaded onto the same column. The enzyme was eluted under isocratic conditions with the same buffer. Under these conditions, the production and purification yields were 100 mg/liter and 80%, respectively. Enzyme purity was verified by SDS-polyacrylamide gel electrophoresis followed by Coomassie Blue and silver staining. The protein concentration was estimated on the basis of the  $A_{280}$  value, and the molar extinction coefficient was from the number of tyrosine and tryptophan residues (19).

**Crystallization and Structure Determination**—Crystals suitable for structure determination were obtained by the hanging drop method. The initial 6- $\mu$ l drop, containing 2.0 mg/ml protein in 45 mM MES buffer at pH 5.25, 5% (w/v) PEG 1500, was equilibrated against 500  $\mu$ l of 200 mM MES buffer containing 20% (w/v) PEG 1500 and 6% (v/v) *n*-propyl

<sup>1</sup> The abbreviations used are: PCR, polymerase chain reaction; IPTG, isopropyl-1-thio- $\beta$ -D-galactopyranoside; MES, 4-morpholineethanesulfonic acid; PEG, poly(ethylene glycol); SIRAS, single isomorphous replacement with anomalous scattering; r.m.s.d., root mean square deviation.

TABLE I  
 Diffraction data, phasing, and refinement statistics

Diffraction data statistics <sup>a</sup>										
Data set	Resolution	Number of observations	Unique reflections	Multiplicity	Bijvoet pairs	$R_{\text{merge}}^b$	Completeness	$\langle I/\sigma I \rangle$	$R_{\text{iso}}^c$	$R_{\text{anom}}^d$
Native 1	31.0–2.9	22,403	6495	3.4		0.029 (0.040)	98.1 (82.7)	47.9 (22.2)		
K <sub>2</sub> PtCl <sub>4</sub>	31.6–2.9	40,484	6494	6.2	5225	0.038 (0.057)	98.4 (88.9)	52.8 (22.9)	0.13	0.027 (0.041)
Native 2	31.0–1.64	111,487	32,628	3.4		0.036 (0.192)	91.9 (68.0)	32.7 (3.2)		
SIRAS phasing statistics										
No. of sites	Occupancy	Anomalous occupancy	$R_{\text{cullis}}$ (acentric/centric)		Anomalous $R_{\text{cullis}}$	Phasing power (acentric/centric)		Figure of merit (acentric/centric)		
1	0.45	0.46	0.52/0.43		0.81	2.4/2.0		0.50/0.51		
Refinement statistics										
Resolution range	No. of reflections	No. of protein atoms	No. of water molecules	$R$ -factor <sup>e</sup>	$R_{\text{free}}$	Average B-factors Å <sup>2</sup>				
						All atoms	Main chain	Side chain	Water	
31.0–1.64	32,628	2024	115	0.192	0.214	13.3	11.4	14.4	22.8	
Geometric parameters r.m.s.d.										
Bond lengths (Å)		Bond angles (°)		Dihedral angles (°)			Improper angles (°)			
0.006		1.30		23.38			1.126			

<sup>a</sup> The numbers given in parentheses denote the respective values of the highest resolution shell.

<sup>b</sup>  $R_{\text{merge}} = \sum \sum |I_i - \langle I_i \rangle| / \sum \sum I_i$ .

<sup>c</sup>  $R_{\text{iso}} = \sum |F_{\text{PH}} - F_{\text{P}}| / \sum |F_{\text{P}}|$ .

<sup>d</sup>  $R_{\text{ano}} = \sum |I^+| - \langle I^+ \rangle / \sum (\langle I^+ \rangle + \langle I^- \rangle)$ .

<sup>e</sup>  $R = \sum |F_o| - |F_c| / \sum |F_o|$ .

alcohol. After 4 days at 22 °C, parallelepipedic crystals and thin plates were formed. Equilibration was pursued for 15 days at 4 °C prior to crystal mounting. The crystals ( $60 \times 100 \times 850 \mu\text{m}^3$ ) belong to the orthorhombic system, space group  $P2_12_12$  with cell parameters  $a = 78.7 \text{ \AA}$ ,  $b = 52.9 \text{ \AA}$ ,  $c = 67.5 \text{ \AA}$ , and contain one molecule in the asymmetric unit. Diffracted synchrotron intensities of both native and derivative crystals were measured on beam line W32 at LURE (Orsay, France) on a large MAR Research imaging plate. The wavelength of the x-ray beam was 0.975 Å. Two crystals were used to collect the native x-ray intensities: one crystal for a 2.9-Å resolution data set and the other one for data to 1.64-Å resolution. The platinum derivative was obtained by soaking the native protein crystals in 3 mM K<sub>2</sub>PtCl<sub>4</sub> for 65 h, and one crystal was used for collecting an anomalous data set to 2.9-Å resolution.

All data were processed using MOSFLM (20). The structure was solved by single isomorphous replacement with anomalous scattering (SIRAS), and the position of the single heavy atom was determined from the Harker sections of the difference Patterson function. Its coordinates and occupancy were refined using MLPHARE (21, 22) on reflections between 31- and 2.9-Å resolution. The SIRAS phases were improved by solvent flattening, histogram matching, and skeletonization with the DM program (22, 23). Refinement, applying a bulk solvent correction with a density of  $0.34 \text{ e}^- \text{ \AA}^{-3}$ , a solvent radius of 0.25 Å and temperature factors of  $50 \text{ \AA}^2$ , with X-PLOR (24) was carried out with no cutoff on diffraction data. In each refinement cycle, manual corrections using the software O (25), were followed by 200 steps of Powell energy minimization of all atoms with harmonic restraints on  $C\alpha$  positions, simulated annealing from 3000 to 300 K (0.5-fs time step), Powell minimization until convergence, and individual B-factor refinement. Electrostatic energy terms were turned off. Water molecules were included so as to account for the positive peaks in the  $|F_{\text{obs}} - F_{\text{calc}}|$  difference Fourier map drawn at 4 S.D. above the mean value, provided they were at hydrogen bond geometry from protein or other solvent atoms. Hereafter, the simulated annealing was performed from 600 to 300 K with a time step of 1 fs. After inclusion of 115 water molecules, the slow cooling scheme was abandoned for conventional refinement that was run until convergence. Grouped occupancies were refined for alternative conformations of Ile-30 C $\delta$ 1 and the Asn-63 side chain.

If not explicitly stated, positional differences given for single residues concern the r.m.s. deviation on all atoms of this residue, whereas differences given for a range of residues concern the r.m.s. deviation on the backbone atoms of these residues. Structure superimpositions were made with ProFit (SciTech Software).

## RESULTS

**Structure Determination**—The completeness, high multiplicity, and low  $R_{\text{merge}}$  values of the data sets proved to be valuable in the phasing procedure (Table I). The quality of the SIRAS phased electron density map computed to a resolution of 2.9 Å allowed an unambiguous main-chain tracing except for residues 100–103 in a loop region and for three residues at the N and C termini. One-third of the side chains were built at this stage. Inclusion of the high resolution data, followed by three rounds of refinement led to  $R$  and  $R_{\text{free}}$  (26) values of 0.230 and 0.253, respectively, at 1.64-Å resolution before inclusion of water molecules. The refined structure of NMC-A includes 265 residues and 115 water molecules, and the final  $R$  and  $R_{\text{free}}$  values for all reflections between 31 and 1.64 Å were 0.192 and 0.214, respectively (Table I). The average temperature factor was  $13.3 \text{ \AA}^2$ , very close to the value estimated ( $13.6 \text{ \AA}^2$ ) from the Wilson plot (27). Coordinate errors were evaluated to be  $0.18 \text{ \AA}$  from a Luzzati plot (28). The N- and C-terminal amino acids and seven solvent-exposed side chains of other amino acids in the sequence showed poorly defined electron densities. Alternative conformations were observed for Ile-30 C $\delta$ 1 and the Asn-63 side chain.

The substrate-binding site is at the interface between two domains. The first one, hereafter denoted as the  $\beta$ -domain (residues 26–60 and 221–291), includes a five-stranded anti-parallel  $\beta$ -sheet (strands S1–S5) and helices H1, H10, and H11. The second one, the helical domain (residues 69–212), is made of eight helices (H2–H9) connected by loop regions (Fig. 2). The overall fold of the protein is similar to that of other class A  $\beta$ -lactamases (29–32), but a number of structural differences were found, particularly in the substrate-binding site. In the following paragraphs, we address the possible functional significance of these differences with respect to the penicillinase, cephalosporinase, and carbapenemase activities of NMC-A.

**The Substrate-binding site**—A specific feature of the class A NMC-A, IMI-1, and Sme-1  $\beta$ -lactamases is the presence of cysteine residues at positions 69 and 238 (Fig. 3) (17). In the NMC-A structure, these cysteines form a left-handed disulfide



FIG. 2. Stereo view of the  $C\alpha$  trace of NMC-A (black) and of TEM-1 (green) after superimposition of the enzyme structures based on the least square minimization of all atoms of the catalytic residues. The r.m.s.d. of all  $C\alpha$  positions of the proteins is 2.6 Å. The first and last residue in each secondary structure element is labeled. The active site serine and the disulfide bridge in NMC-A are shown in bold.

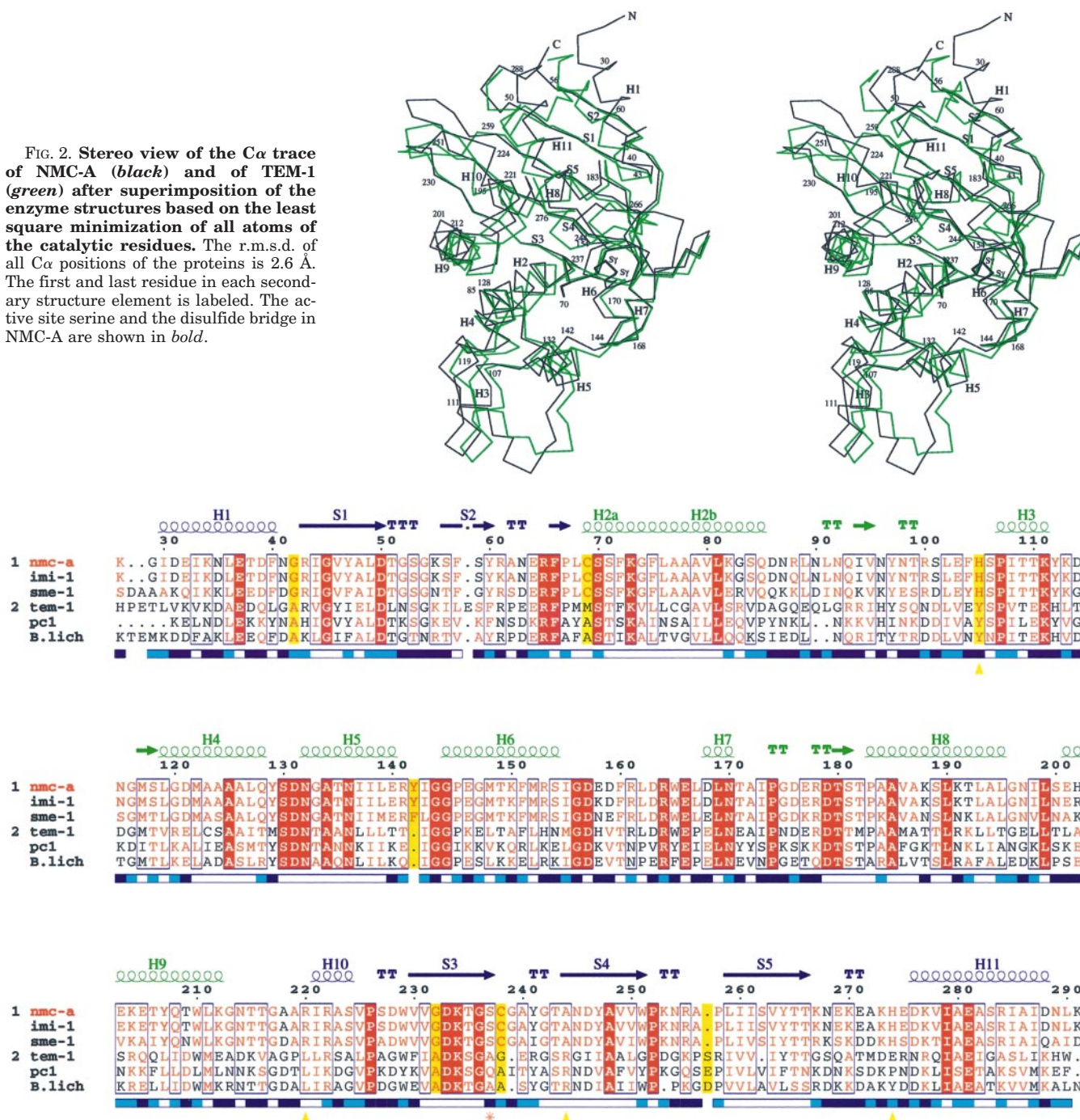


FIG. 3. Sequence alignment of the three class A carbapenemases (labeled as group 1) and of the typical class A  $\beta$ -lactamases (group 2) for which coordinates are available (Protein Data Bank, Brookhaven National Laboratory, codes: 1BTL, 3BLM, and 4BLM, respectively). The secondary structure elements (top) and the solvent accessibilities (bottom) in NMC-A are shown. The color code used is: accessible (dark blue), intermediate (light blue), and buried (white). Strictly conserved residues (red boxes), homologous residues in each group (red characters), homologous residues in both groups (blue boxes), and variations detected from sequence homology matrices (yellow boxes) are shown. Residues indicated by triangles and stars are discussed in the text. This figure was produced by ESPript (P. Gouet and F. Métoz, to be published; available through FTP anonymous at ftp.ipbs.fr).

bridge, with a  $C\beta$ - $S\gamma$ - $S\gamma$ - $C\beta$  dihedral angle of  $-103.4^\circ$  and a  $C\alpha$ - $C\alpha$  distance of 5.0 Å. This covalent bond links the N terminus of helix H2 (containing the catalytic Ser-70 residue) to strand S3 (230–237), which defines one side of the substrate-binding site (Fig. 4). The disulfide bridge has several consequences. First, this bond and the set of interactions shown in Fig. 5, would be expected to greatly diminish structural flexibility in this region of the structure. Second, the distance between the main-chain nitrogen atoms of residues 70 and 237, which define the oxanion hole, is 0.3 Å shorter than the

average value (4.7 Å) in other class A  $\beta$ -lactamases (33). This would result in somewhat stronger hydrogen bonding of the water molecule typically found in that position in the absence of substrate. Finally, residue 238 adopts a conformation in which its carbonyl group is flipped by  $180^\circ$  from the corresponding position seen in all other structures of class A  $\beta$ -lactamases. As a consequence, the S3 strand breaks from Ser-237, and the infrequent glycine residue inserted at position 239 moves away from the  $\Omega$  loop region.

Several polar side chains are oriented toward the substrate-

FIG. 4. **Stereo view of the NMC-A substrate-binding site.** The color code used is: oxygen (red), carbon (yellow), nitrogen (blue), and sulfur (green). The water molecules are shown as red spheres. The salt-bridge interaction between Arg-100 and Asp-103 is indicated.

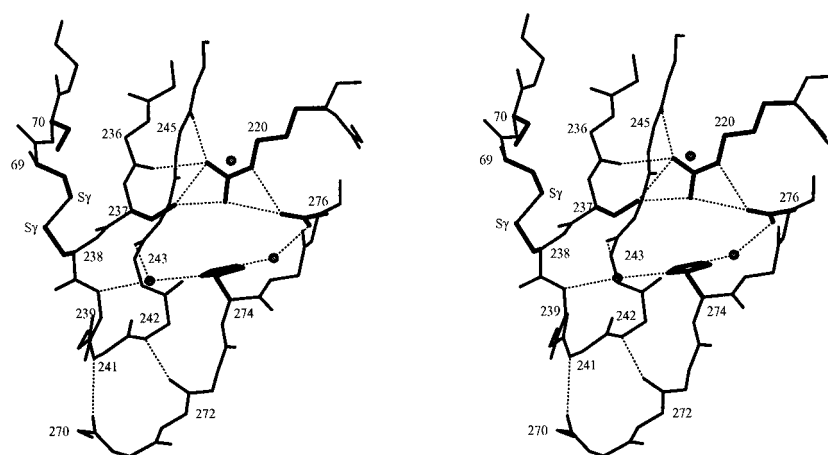
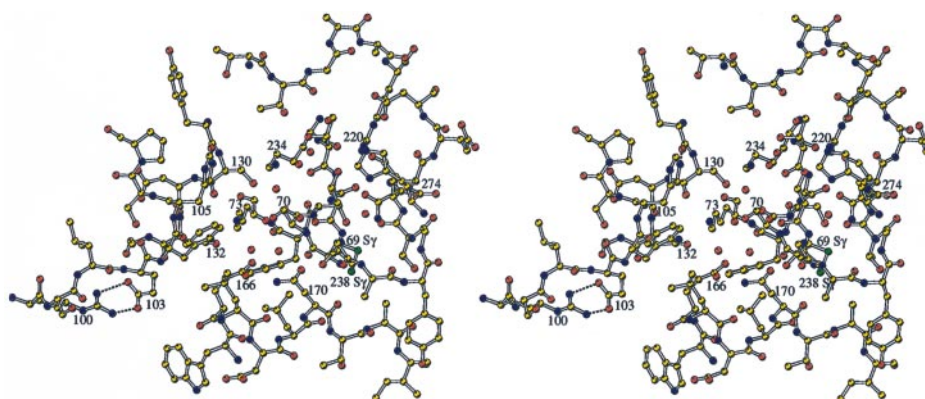


FIG. 5. **Stereo view of the hydrogen bond pattern (dotted lines) involving Arg-220 and His-274 in the NMC-A structure.** Water molecules are indicated by spheres.

binding site (Fig. 4). The uncommon histidine residues at positions 105 and 274 face each other at the entrance of the active site cavity. The side chain of His-274 is hydrogen bonded through one water molecule to the acidic group of Asp-276 and through a second water molecule to the main-chain nitrogen and oxygen atoms of residues 239 and 243, respectively (Fig. 5). At van der Waals distance from His-274, the guanidinium group of Arg-220 is engaged in a set of interactions that likely decrease its mobility and effective charge. It forms a salt-bridge interaction with Asp-276 and is hydrogen bonded to the main-chain oxygen atoms of residues 236 and 245, and to the hydroxyl group of Ser-237 (Fig. 5). The guanidinium group is located in an area similar to that of Arg-244 in the *E. coli* TEM-1  $\beta$ -lactamase (32), in which it interacts with the carboxylate group of the substrate in the x-ray structures of acyl-enzyme complexes (31, 34, 35).

The disulfide bridge between cysteines 69 and 238 does not seem to affect the catalytic machinery of the protein (Table II). All atoms of the conserved catalytic residues (Ser-70, Lys-73, Ser-130, Glu-166, and Lys-234; 39 atoms) in NMC-A are found in the same positions as in typical class A enzymes. A least square fit of these atoms from the *Staphylococcus aureus* PC1 (29), *Bacillus licheniformis* 749/C (30), and *E. coli* TEM-1 (32) enzymes gives an r.m.s.d. of 0.3 Å, and the same result is obtained when NMC-A is also included in the calculation. We applied the corresponding transformation matrices to all protein atoms to compare the environment of these catalytic residues and the substrate-binding sites in the superimposed protein structures (Fig. 6, A and B). We observed that the atomic positions of Asn-132, which were not taken into account to compute the superimposition matrices, were similar (r.m.s.d. = 0.2 Å) in the three enzymes devoid of carbapenemase activity but are shifted by 1.0 Å in NMC-A, when compared with their average positions in the typical class A enzymes. This differ-

TABLE II  
Distances in the active-site cleft

Identification <sup>a</sup>	Distance (Å)	
	NMC-A	TEM-1
Ser-70 O $\gamma$	Lys-73 N $\zeta$	2.9
	Ser-130 O $\gamma$	3.1
	Wat-308 <sup>b</sup>	2.5
	Wat-332 <sup>c</sup>	2.7
Lys-73 N $\zeta$	Ser-130 O $\gamma$	3.1
	Asn-132 O $\delta$ 1	2.8
	Glu-166 O $\epsilon$ 1	3.4
	Lys-234 N $\zeta$	5.6
Ser-130 O $\gamma$	Lys-234 N $\zeta$	3.0
	Gly-236 C $\alpha$	10.7
	Ser-237 N	9.8
	Ser-237 O	8.2
Glu-166 O $\epsilon$ 1	Water 332 <sup>c</sup>	2.6
	Asn-170 N $\delta$ 2	3.0
	Water 332 <sup>c</sup>	2.6
	Ser-70 N	3.0
Water 308 <sup>b</sup>	Ser-237 N	2.8
	Ser-237 O	2.6
	Ser-70 N	3.1
	Ser-237 N	4.4

<sup>a</sup> Residue name as in NMC-A.

<sup>b</sup> Located in the oxyanion hole.

<sup>c</sup> The catalytic water molecule involved in deacylation.

ence does not arise from a local displacement of the H5 helix (residues 132–142), but seems to result from folding variations throughout the protein structure (Fig. 2). It was also apparent that the main-chain oxygen atom of Ser-237, which was shown to interact with the nitrogen atom of the 6 $\beta$ -acylamido substituent of penicillin substrates during catalysis (31), is displaced by 1.0 Å compared with the PC1 and TEM1 enzymes (Fig. 6, A and B). This movement likely results from the  $\alpha$ -conformation adopted by residue 238 but seems unrelated to the insertion at



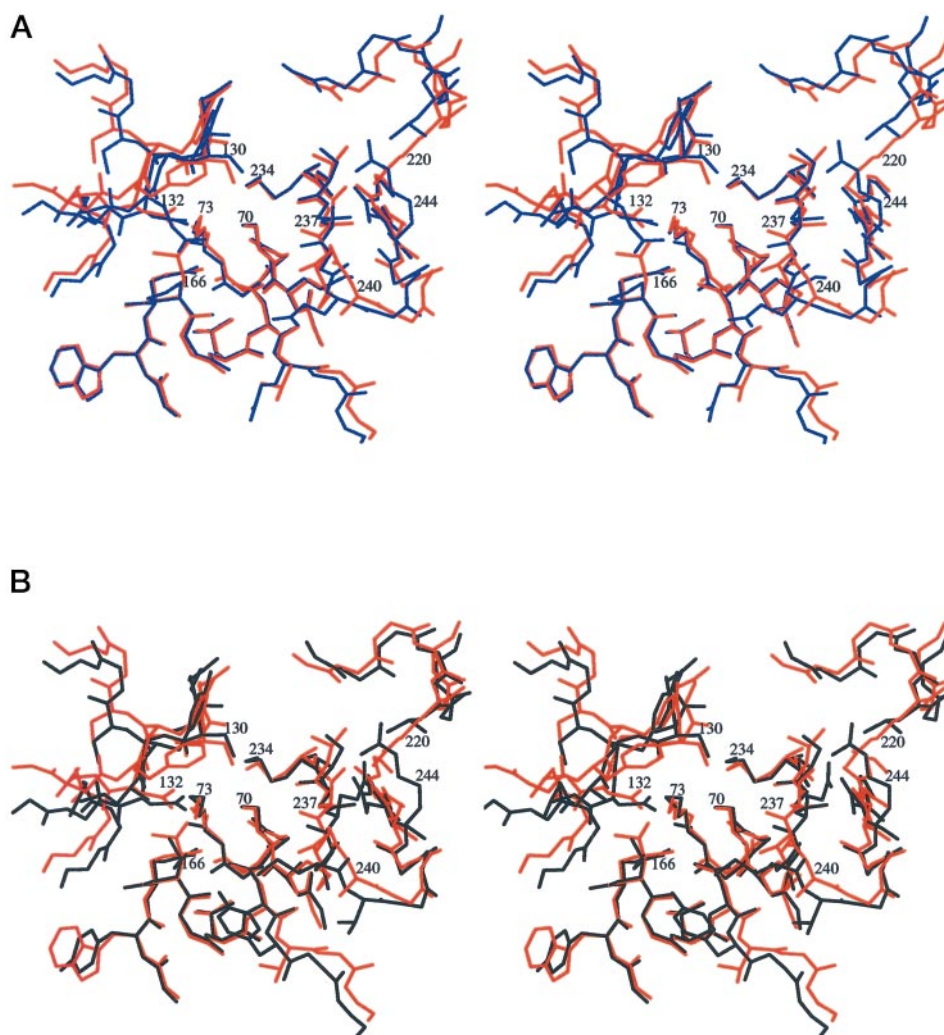


FIG. 6. **Stereo view of the substrate-binding sites in class A enzymes.** The superimposition of the enzyme structures is based on the least square minimization of all atoms from the catalytic residues (see text). A, NMC-A (red) and TEM-1 (blue); B, NMC-A (red) and PC1 (black).

position 239. Indeed, compared with the TEM-1 (32) and *B. licheniformis* (30) class A enzymes, the position of the main-chain oxygen atom of residue 237, and the conformation of residue 238 are not affected in the PC1  $\beta$ -lactamase (29) although this enzyme contains an isoleucine inserted at position 239. The 237–240 regions in NMC-A and PC1 differ significantly (r.m.s.d. = 1.5 Å) (Fig. 6B), which suggests that the specific conformation of the C-terminal edge of the S3 strand in NMC-A may be attributed to the presence of the disulfide bridge. Cysteine 69 belongs to the polypeptide stretch connecting the  $\alpha$  and  $\beta$  domains of the protein. Formation of the disulfide bridge may influence the relative orientation of these domains and contribute to the folding variations illustrated in Fig. 2.

#### DISCUSSION

NMC-A and the class A  $\beta$ -lactamases devoid of carbapenemase activity are similar with respect to their hydrolytic machinery. The positions of the essential catalytic residues are identical within a r.m.s.d. of 0.3 Å, a value close to the estimated coordinate errors of 0.2 Å in structures refined below 2-Å resolution. This similarity, which preserves the molecular bases of the catalytic mechanism (36, 37), is in line with the high penicillinase activity of NMC-A.

On the contrary, we observed specific positional differences at residues 132 and 237–240. Several studies have emphasized the implication of the 238–240 region, at the edge of the sub-

strate-binding site, with respect to the improved hydrolysis of third-generation cephalosporins and monobactams, by class A enzymes with extended-substrate specificity. An enhanced recognition of cephalosporins was displayed by engineered *S. aureus* PC1 enzymes (A238S and Ile-239 deleted;  $\Omega$ -loop deletion), and the x-ray structures revealed an altered disposition of the C-terminal edge of the S3 strand (38, 39). Several investigations were reported on the TEM and SHV enzymes because mutations naturally occurring in that region have been found in proteins responsible for bacterial resistance to  $\beta$ -lactam antibiotics (40). It was pointed out that the size correlation between the side chains of residues 69 and 238 in the parent enzymes breaks down in extended-spectrum  $\beta$ -lactamases, and it was suggested that the steric constraints would be accommodated by pushing the lower part of the S3 strand away from the active site, by 1–2 Å (41). In NMC-A, although the disulfide bridge reduces the  $C\alpha$ - $C\alpha$  distance between residues 69 and 238, the conformation adopted by Cys-238 induces the predicted distortion in this part of the strand. It increases the space available between residue 170 of the  $\Omega$  loop region and the S3 strand, where the large 7 $\beta$  substituents of third-generation cephalosporins were reported to bind (39, 41, 42). The inserted glycine 239 ( $\Phi = 78^\circ$ ,  $\Psi = 18^\circ$ ), with its large available conformational space, might help to satisfy the constraints associated to the formation of the adjacent disulfide bridge. In addition, the side chain of any other residue in that position

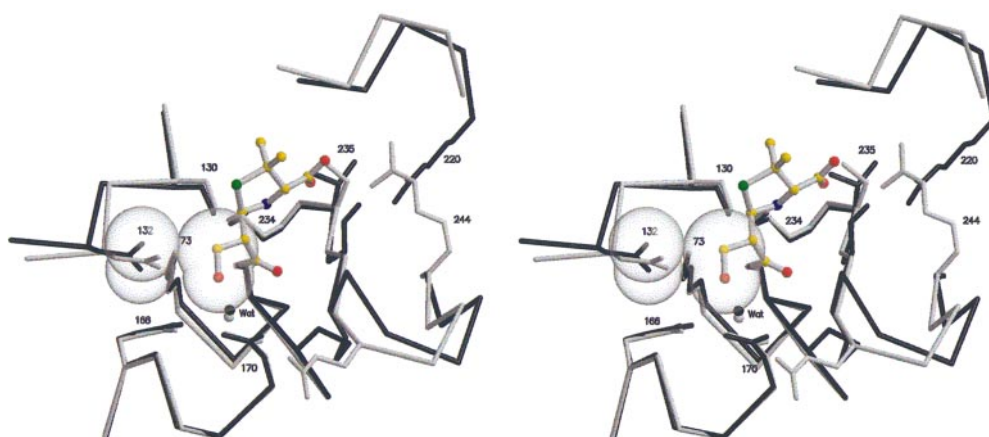


FIG. 7. Superimposition of NMC-A (black) and of the acyl-enzyme complex TEM-1-6 $\alpha$ -hydroxymethyl penicillanic acid (gray) (34) based on the least square minimization of all atoms from the catalytic residues. The van der Waals spheres corresponding to Asn-132 O $\delta$ 1 and N $\delta$ 2 in NMC-A, and to the 6 $\alpha$ -hydroxymethyl group, are shown. It illustrates that several positions of the hydroxyl group may be accommodated in NMC-A ( $k_{\text{cat}}/K_m = 10^5 \text{ M}^{-1} \text{ s}^{-1}$ ), in contrast to the situation in the inhibited TEM-1 enzyme in which it could only be oriented toward the deacylating water molecule (black and gray spheres).

would be oriented toward the binding site and would counteract the effect promoted by the conformation of residue 238.

With respect to the hydrolytic properties of NMC-A with carbapenem and cephamycin substrates, the direct implications of the disulfide-linked Cys-238 cannot be foreseen from the x-ray structure. The residues in the 238–240 region do not provide direct binding interactions to the functionalities on the  $\alpha$  face of the substrate, such as the 6 $\alpha$ -hydroxyethyl group of carbapenem antibiotics. It is noteworthy that the expanded-substrate enzymes deriving from the TEM and SHV  $\beta$ -lactamases, which display mutations of these residues, have not been reported to hydrolyze carbapenems and cephamycins. The position of Asn-132, away from strand S3 but still at 2.8 Å from Lys-73 N $\zeta$  (Table II) (43), is unusual when compared with any other class A  $\beta$ -lactamase. Its new location might play a major role with respect to the carbapenemase activity because additional space is provided in a critical area for protein-substrate interactions, which would permit accommodating the 6 $\alpha$ -1R-hydroxyethyl substituent of carbapenems. This proposal is supported by kinetic and structural data. Mobashery and co-workers (44) showed that the attenuation of the turnover rate of imipenem with the TEM-1 enzyme only arises, for steric reasons, from the 6 $\alpha$ -1R-hydroxyethyl group and that this group imparts resistance to turnover by TEM-1 by  $10^4$ -fold. These data were in line with the observations made from the crystal structure of the acyl-enzyme complex formed between TEM-1 and its inhibitor, 6 $\alpha$ -hydroxymethyl penicillanic acid, solved at 2.0-Å resolution (34). The three-dimensional structure showed tight interactions between the inhibitor, Asn-132, and strand S3 and indicated that the larger 6 $\alpha$ -1R-hydroxyethyl group of carbapenems would induce steric clashes with residue 132. The superimposition of the TEM-6 $\alpha$ -hydroxymethyl penicillanic acid and NMC-A structures, based on the best fit of the atoms of their catalytic residues (Fig. 7), suggested that the 1.0-Å displacement of Asn-132 away from strand S3 in NMC-A (Table II), would allow the 6 $\alpha$ -hydroxymethyl substituent to be easily accommodated and the hydroxyl group to orient differently in NMC-A. Indeed, kinetic experiments indicated a  $k_{\text{cat}}/K_m$  value of  $10^5 \text{ M}^{-1} \text{ s}^{-1}$  for this substrate (detailed kinetic studies will be presented elsewhere).

In the TEM-1-penicillin G acyl-enzyme complex (31), the oxygen and nitrogen atoms of the 6 $\beta$ -acylamido group of the substrate were found at 2.6 Å from Asn-132 N $\delta$ 2 and at 2.9 Å from the main-chain oxygen of residue 237, respectively. The altered position of this atom, and its increased distance to Asn-132 N $\delta$ 2 in NMC-A (Table II), suggested that this hydro-

gen bond pattern may be altered in this enzyme with penicillin substrates. To evaluate this hypothesis, we determined the  $k_{\text{cat}}/K_m$  value for 6 $\beta$ -aminopenicillanic acid that, from its chemical structure, may only interact with the main-chain oxygen atom of residue 237. We found that the hydrolytic efficiency for this substrate by NMC-A was similar, within experimental errors, to that for penicillin G, suggesting that in this enzyme the interaction between the oxygen atom of the 6 $\beta$ -acylamido group of penicillin G and Asn-132 may be weakened.

The most prominent features in the substrate-binding site of NMC-A are the altered conformations at the edge of the S3 strand and the unusual position of Asn-132. The former is reminiscent of several observations made to explain the extended-spectrum activity of typical class A mutant enzymes. The position of Asn-132 seems to be important for catalytic efficiency against  $\beta$ -lactam antibiotics bearing a 6 $\alpha$  substituent (carbapenems), and both 7 $\alpha$  and 7 $\beta$  substituents (cephamycins).

From the clinical point of view, the gene encoding NMC-A is derived from a member of the *Enterobacteriaceae* family, which is a common source of nosocomial infections for which carbapenems are often the  $\beta$ -lactams of last resort for use in patients in intensive care units. The broad substrate specificity of NMC-A, together with the poor effect of the inhibitors of class A enzymes currently in therapeutic use, should stimulate the design of new structure- and mechanism-based inhibitors, as was successfully done with the TEM-1 enzyme (34, 35).

#### REFERENCES

- Bush, K., Jacoby, G. A., and Medeiros, A. A. (1995) *Antimicrob. Agents Chemother.* **39**, 1211–1233
- Edwards, J. R. (1995) *J. Antimicrob. Chemother.* **36**, Suppl. A, 1–17
- Blumer, J. L. (1995) *Scand. J. Infect. Dis. Suppl.* **96**, 38–44
- Labia, R., Morand, A., Tiwari, K., Sirot, D., and Chanal, C. (1989) *J. Antimicrob. Chemother.* **24**, Suppl. A, 219–223
- Galleni, M., Amicosante, G., and Frère, J. M. (1988) *Biochem. J.* **255**, 123–129
- Taibi, P., and Mobashery, S. (1995) *J. Am. Chem. Soc.* **117**, 7600–7605
- Yang, Y., Bhachech, N., and Bush, K. (1995) *J. Antimicrob. Chemother.* **35**, 75–84
- Livermore, D. M. (1992) *J. Antimicrob. Chemother.* **29**, 609–613
- Felici, A., and Amicosante, G. (1995) *Antimicrob. Agents Chemother.* **39**, 192–199
- Carfi, A., Pares, S., Duee, E., Galleni, M., Duez, C., Frère, J. M., and Dideberg, O. (1995) *EMBO J.* **14**, 4914–4921
- Concha, N. O., Rasmussen, B. A., Bush, K., and Herzberg, O. (1996) *Structure (Lond.)* **4**, 823–836
- Nordmann, P., Mariotte, S., Naas, T., Labia, R., and Nicolas, M. H. (1993) *Antimicrob. Agents Chemother.* **37**, 939–946
- Rasmussen, B. A., Bush, K., Keeney, D., Yang, Y., Hare, R., O'Gara, C., and Medeiros, A. A. (1996) *Antimicrob. Agents Chemother.* **40**, 2080–2086
- Naas, T., Vandel, L., Sougakoff, W., Livermore, D. M., and Nordmann, P. (1994) *Antimicrob. Agents Chemother.* **38**, 1262–1270
- Rasmussen, B. A., and Bush, K. (1997) *Antimicrob. Agents Chemother.* **41**, 223–232



16. Mariotte-Boyer, S., Nicolas-Chanoine, M. H., and Labia, R. (1996) *FEMS Microbiol. Lett.* **143**, 29–33
17. Raquet, X., Lamotte-Brasseur, J., Bouillenne, F., and Frère, J. M. (1997) *Proteins Struct. Funct. Genet.* **27**, 47–58
18. Sougakoff, W., Jarlier, V., Delettré, J., Colloc'h, N., L'Hermite, G., Nordmann, P., and Nass, T. (1996) *J. Struct. Biol.* **116**, 313–316
19. Cantor, C. R., and Schimmel, P. R. (1980) *Biophysical Chemistry*, pp. 374–385, W. H. Freeman and Co., New York
20. Leslie, A. G. W. (1987) *Computational Aspects of Protein Crystal Data Analysis, Proceedings of the Daresbury Study Weekend* (Helliwell, J. R., Machin, P. A., and Papiz, M. Z., eds.) pp. 39–50, SERC, Daresbury Laboratory, Warrington, United Kingdom
21. Otwinowski, Z. (1991) *Isomorphous Replacement and Anomalous Scattering, Proceedings of the CCP4 Study Weekend* (Wolf, W., Evans, P. R., and Leslie, A. G. W., eds) pp. 80–86, SERC, Daresbury Laboratory, United Kingdom
22. Collaborative Computational Project, Number 4 (1994) *Acta Crystallogr. Sec. D* **50**, 760–763
23. Cowtan, K. D. (1994) *Joint CCP4 and ESF-EACBM Newsletter on Protein Crystallography* (Bailey, S., and Wilson, K., eds) pp. 34–38 Daresbury Laboratory, Warrington, United Kingdom
24. Brünger, A. T. (1992) *X-PLOR Version 3.1, A System for X-ray Crystallography and NMR*, Yale University Press, New Haven, CT
25. Jones, T. A., Zou, J. Y., Cowan, S. W., and Kjeldgaard, M. (1991) *Acta Crystallogr. Sec. A* **47**, 110–119
26. Brünger, A. T. (1992) *Nature* **355**, 472–475
27. Wilson, A. J. C. (1949) *Acta Crystallogr.* **2**, 318–321
28. Luzzati, V. (1952) *Acta Crystallogr.* **5**, 802–810
29. Herzberg, O. (1991) *J. Mol. Biol.* **217**, 701–719
30. Knox, J. R., and Moews, P. C. (1991) *J. Mol. Biol.* **220**, 435–455
31. Strynadka, N. C. J., Adachi, H., Jensen, S. E., Johns, K., Sielecki, A., Betzel, C., Sutoh, K., and James, M. N. G. (1992) *Nature* **359**, 700–705
32. Jelsch, C., Mourey, L., Masson, J. M., and Samama, J. P. (1993) *Proteins* **16**, 364–383
33. Knox, J. R., Moews, P. C., and Frère, J. M. (1996) *Chem. Biol. (Lond.)* **3**, 937–947
34. Maveyraud, L., Massova, I., Birck, C., Miyashita, K., Samama, J. P., and Mobashery, S. (1996) *J. Am. Chem. Soc.* **118**, 7435–7440
35. Strynadka, N. C. J., Martin, R., Jensen, S. E., Gold, M., and Jones, J. B. (1996) *Nat. Struct. Biol.* **3**, 688–695
36. Maveyraud, L., Chen, C. C. H., Banerjee, S., Li, Z., Wäsch, S., Kapadia, G., Moul, J., and Herzberg, O. (1996) *Biochemistry* **35**, 16475–16482
37. Maveyraud, L., Pratt R. F., and Samama, J. P. (1998) *Biochemistry* **37**, 2622–2628
38. Zawadzke, L. E., Smith, T. J., and Herzberg, O. (1995) *Protein Eng.* **8**, 1275–1285
39. Banerjee, S., Pieper, U., Kapadia, G., Pannell, L. K., and Herzberg, O. (1998) *Biochemistry* **37**, 3286–3296
40. Knox, J. R. (1995) *Antimicrob. Agents Chemother.* **39**, 2593–2601
41. Hutlesky, A., Knox, J. R., and Levesque, R. C. (1993) *J. Biol. Chem.* **268**, 3690–3697
42. Raquet, X., Lamotte-Brasseur, J., Fonze, E., Goussard, S., Courvalin, P., and Frère, J. M. (1994) *J. Mol. Biol.* **244**, 625–639
43. Osuna, J., Viadiu, H., Fink, A. L., and Soberon, X. (1995) *J. Biol. Chem.* **270**, 775–780
44. Miyashita, K., Massova, I., and Mobashery, S. (1996) *Bioorg. Med. Chem. Lett.* **6**, 319–322

**X-ray Analysis of the NMC-A  $\beta$ -Lactamase at 1.64-Å Resolution, a Class A Carbapenemase with Broad Substrate Specificity**

Peter Swarén, Laurent Maveyraud, Xavier Raquet, Stéphanie Cabantous, Colette Duez, Jean-Denis Pédelacq, Sophie Mariotte-Boyer, Lionel Mourey, Roger Labia, Marie-Hélène Nicolas-Chanoine, Patrice Nordmann, Jean-Marie Frère and Jean-Pierre Samama

*J. Biol. Chem.* 1998, 273:26714-26721.

doi: 10.1074/jbc.273.41.26714

---

Access the most updated version of this article at <http://www.jbc.org/content/273/41/26714>

Alerts:

- [When this article is cited](#)
- [When a correction for this article is posted](#)

[Click here](#) to choose from all of JBC's e-mail alerts

This article cites 37 references, 10 of which can be accessed free at <http://www.jbc.org/content/273/41/26714.full.html#ref-list-1>